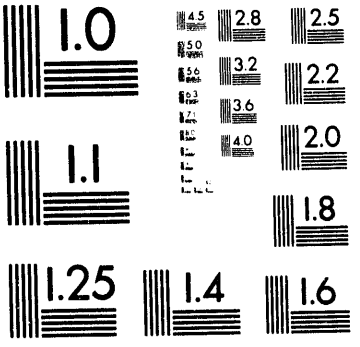
1.0
1.1
1.25
1.4
1.6
1.8
2.0
2.2
2.5
2.8
3.2
3.6
4.0
4.5
5.0
5.6
6.3
7.1

1 of 1

Photopumped X-ray Laser Research on Saturn

T.J. Nash, R.B. Spielman, M. Vargas, and L. Ruggles
Sandia National Laboratories, Albuquerque, NM, 87185

ABSTRACT

Using Saturn as a driver, we are pursuing both photoresonantly pumped and photoionization/recombination lasers. Our lasing targets are gas cells with thin windows that are pumped by a z pinch 2 cm away radiating 10 TW. In both schemes the lasant and gas fill is neon. We will present evidence for inversion in the sodium/neon photoresonant scheme but we have yet to detect the lasing transition itself. To increase our chances of measuring this line we have introduced potassium into a sodium z-pinch and have eliminated oxygen from the gas cell windows. We have measured the spatial dependence of ionization balance across the gas cell, and this measurement is consistent with propagation of a shock front across the gas cell target. We have measured the Li-like neon 5f-3d transition to increase more rapidly with fill pressure than all other measured lines. Based on this result we have performed experiments emphasizing the photoionization/recombination laser scheme that use a flat-field grazing incidence spectrometer to provide good spatial resolution of the 4f-3d, 4d-3p, and 5f-3d lines of Li-like neon. We have attempted a gain length measurement by imaging parallel to a baffle that varies the length of the target illuminated.

1. INTRODUCTION

X-ray lasers demonstrated to date have been pumped by collisional excitation and recombination. [1-10] Although resonant photopumping could potentially produce an efficient x-ray laser [11-20], the shortest wavelength at which photopumped gain has been measured is 2163 Å in Be-like C. [21]

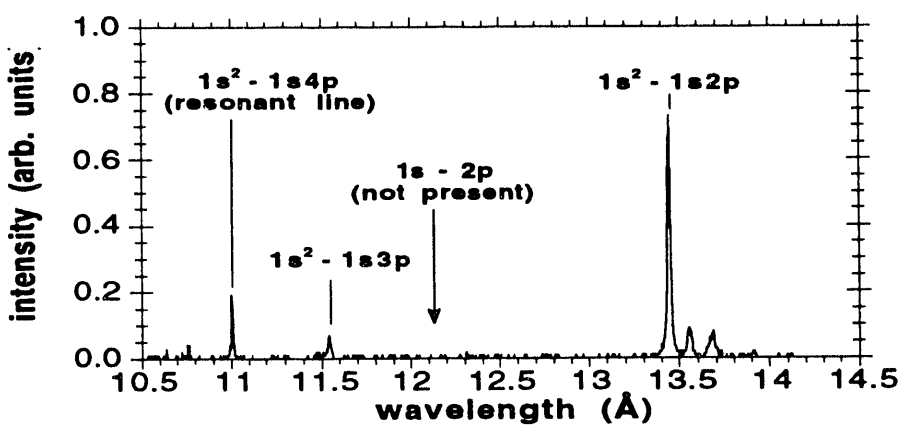

Figure 1. The 4 to 1 line of He-like neon is measured to be twice the intensity of the 3 to 1 line indicating a 4 to 3 inversion.

Using elliptical crystal spectroscopy, resonant photopumping of the n=4 level of He-like neon by a sodium z pinch on the pulsed power driver Saturn has been demonstrated. [22] The measured neon K shell spectrum showing the 4 to 3 inversion in He-like neon is reviewed

in figure 1. The 200-GW pump is sufficient to produce a measureable 4 to 3 inversion in He-like neon. Details are presented in Reference 22. The next logical step in this x-ray laser research is to measure the strongest predicted laser transition, the 4f-3d singlet line at 231 Å.

The atomic energy level diagram including the coincident lines for the sodium/neon x-ray laser scheme is shown in figure 2a. The resonant photopump of typically 200 GW in the He-like sodium 2 to 1 transition is provided by the z pinch load of the Saturn accelerator. Saturn also emits up to 10-TW of total radiation which photoionizes the neon L-shell in the neon lasant target, and is predicted to drive a shock wave from the side window of the gas cell into the neon. [23] The 4p singlet level of He-like neon is resonantly photopumped. Electron and ion collisions distribute the population and hence the 4 to 3 inversion over the n=4 sublevels and the largest gain is predicted for the 4f to 3d singlet transition at 231 Å. [13,19]

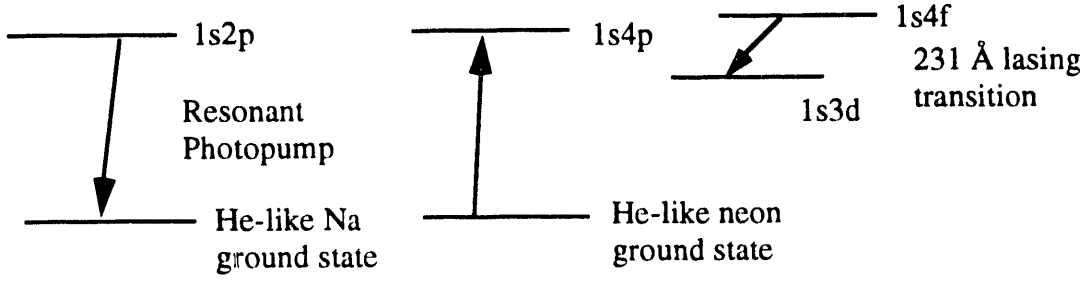

Figure 2a. Atomic energy level diagram for the resonanatly photopumped sodium/neon x-ray laser scheme.

Figure 2b shows the grotian diagram for the photoionization/recombination x-ray laser scheme. This scheme is more versatile in that is does not require a resonant pump and thus several combinations of pump and lasant are possible. It also uses a more significant fraction of the pinch radiation in the pumping.

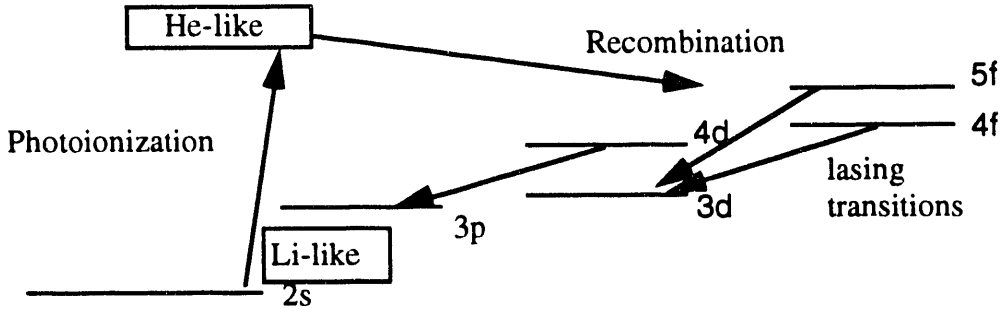

Figure 2b. Atomic energy level Diagram for the Photoionization/Recombination laser schemes.

The experimental arrangement is shown in figure 3. Saturn delivers approximately 10 MA with a 60 nsec rise time to a sodium z pinch load. The pinch radiates up to 10 TW with 200 GW in the resonant photopump. The pulsewidth of the resonant photopump is 20 to 30 nsec. A neon gas cell is placed with its side window 18 mm from the pinch axis, just outside of the pinch current return posts. A typical neon fill pressure of 10 torr is confined by a 4000-Å thick Lexan side window and an end window that is either 2000-Å thick Lexan or 5000-Å thick polystyrene. The pumping radiation is incident on and ionizes the side window, and also

heats the neon gas target. XUV radiation is measured along an axial line of sight passing through the end window with a spatially resolved 10-nsec gated MCPIGS (microchannel plate (MCP) intensified one meter grazing incidence spectrometer).[24] The XUV radiation has also been measured by a flat field variable line spaced grazing incidence grating spectrometer that has spectral and spatial resolution superior to the MCPIGS.

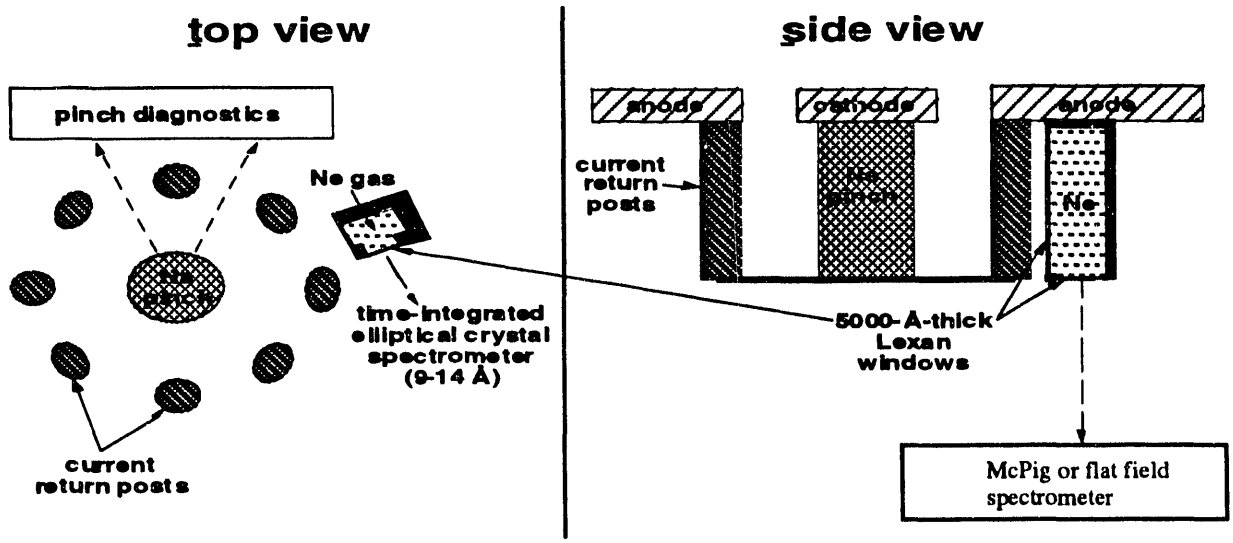

Figure 3. Experimental Arrangement

2. INSTRUMENTATION

We measure the XUV spectra from the neon gas cell with a spatially resolved single time-gated MCPIGS. The MCP is curved to the one meter diameter of the Rowland circle. The instrumental acceptance is f/40 up to a 3-meter radius 2-degree grazing incidence spherical gathering mirror. A 6-mm wide by 150-mm long stripline on the MCP is gated by a 10-nsec 900-volt pulse to provide a single 10-nsec resolved time frame. Typically the gate is centered on the peak of the z pinch x-ray emission. On the short 6-mm width of the strip we spatially resolve with an imaging cylindrical mirror at 5-degrees grazing incidence. With spatial magnification of 1/2.7 the spatial resolution at the target is better than 1-mm. However due to the large 150-mm length of the spectral focus, the spatial focus degrades rapidly away from the spatial focus wavelength. At spectral locations 15-Å from the spatial focus, the spatial resolution degrades to worse than 1-mm. On the MCPIGS instrument we use two vacuum spacers, one for spatial focus at 230-Å and one for spatial focus at 80-Å, assuming the use of a typical 1200 l/mm grating. For the spatial focus at 230-Å we use a 1200 l/mm grating blazed at 5-degrees, and a 1000-Å Al filter to remove higher orders. For spatial focus at 80-Å we use no filter and a 1200-l/mm grating blazed at 2-degrees. The entrance slit width is typically 20-microns and the grating is half masked. A spherical spectral gathering mirror sets the field of view as 1 mm wide at the gas cell, the other dimension of the gas cell being imaged by the cylindrical mirror. A closed to closed fast valve with 3-mm by 3-cm aperture open for 500-microseconds protects the mirrors from shot debris. The microchannel plate is backed by a fiber optic faceplate coated with P11 phosphor. The spectral data is recorded on Kodak type 2484 film, then digitized and computer processed.

We have addressed the limitation in the spatial imaging of the MCPIGS by using a flat field variable line spaced grating spectrometer that maintains spatial focus along the entire

spectral range. This instrument also has spectral resolution superior to the MCPIGS, and this has revealed useful information on line shapes to be discussed in the results section. The flat field instrument uses no spectral gathering mirror as we deployed it. Its field of view, unlike the MCPIG, includes the entire 6-mm diameter of the gas cell end window. We have found that because of the increased throughput of the flat field spectrometer it was necessary to use a 2000-Å thick aluminum filter to remove higher orders from the vicinity of candidate laser transitions.

3. RESULTS

An attempt at measuring the 231-Å line is depicted in figure 4. When viewed through a 2000-Å thick lexan end window the spectrum is plagued with oxygen absorption lines, one of which falls precisely on the location of the resonantly photopumped laser line. We eliminated these oxygen lines by using a 5000-Å oxygen-free polystyrene end window. With this end window the oxygen absorption lines disappear and the background level, likely due to oxygen lines as well as continuum emission, is reduced. Estimates of instrumental sensitivity and fluorescent yield in the laser line indicate that we are unlikely to detect the 231-Å transition unless it is lasing with a gain greater than 1 cm^{-1}.

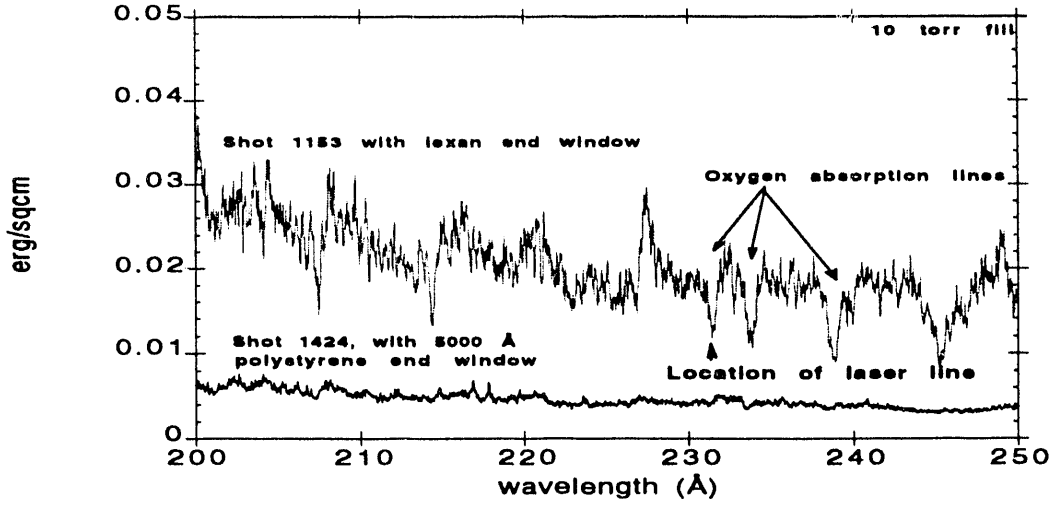

Figure 4. A polystyrene end window eliminates oxygen absorption.

Measurements of ionization balance are made by recording spectra in the 70 to 120-Å window. This region includes bright 3 to 2 transitions in Be-like, Li-like, and He-like neon. With a pure sodium z-pinch pump the lines of Be-like and Li-like neon are about equal as depicted in the bottom trace of figure 5. One reason we are not detecting the laser line could be a paucity of He-like neon. Complete photoionization of the neon L-shell requires copious radiation at 240 to 450-eV energies, and a sodium plasma is lacking in transitions near these energies. In order to increase the photoionization pump we introduce potassium into the z pinch with the idea that potassium L radiation could help photoionize the neon L shell and produce more He-like neon. With 25% potassium in the driving pinch the ratio of Li-like to Be-like neon line intensities increases a factor of 2 indicating a higher ionization level and thus more He-like neon is present when potassium is used in the pinch.

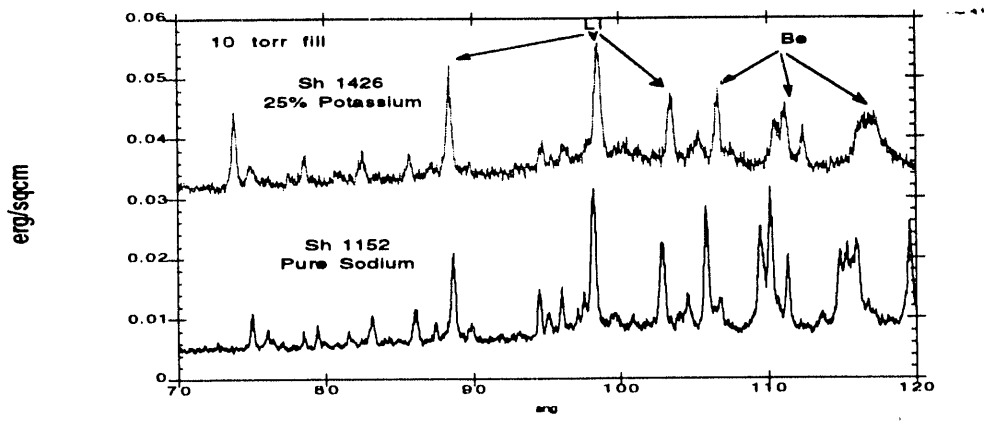

Figure 5. 25% potassium in the sodium pinch increases the neon ionization state.

The effect of different amounts of potassium introduced into the sodium pinch was scanned on a shot to shot basis. The results are shown in figure 6. The total number of wires in the z pinch load array is 16. The power in the 250 to 450 eV window is measured by a titanium-filtered carbon x-ray diode. This diode in figure 6 shows the power in this window increasing a factor of 3 in going from 0 to 25% potassium in the load. The 11-Å resonant photopump line power and total sodium K-shell power, measured by x-ray diodes, bolometers, and photoconductive detectors, do not significantly decrease up to a 25% fraction (4 wires) of potassium. However at 50% potassium (8 wires) the sodium K shell and resonant photopump power fall off dramatically. The data of figure 6 shows that 25% potassium in the sodium load optimizes the ability of the z pinch to both photoionize the neon L shell and resonantly photopump the He-like neon.

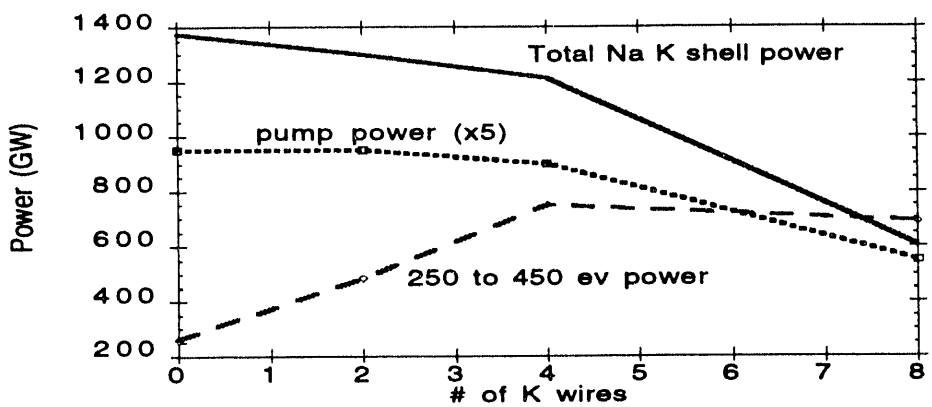

Figure 6. The optimum amount of potassium in the sodium pinch is 4 wires or 25% of the total mass.

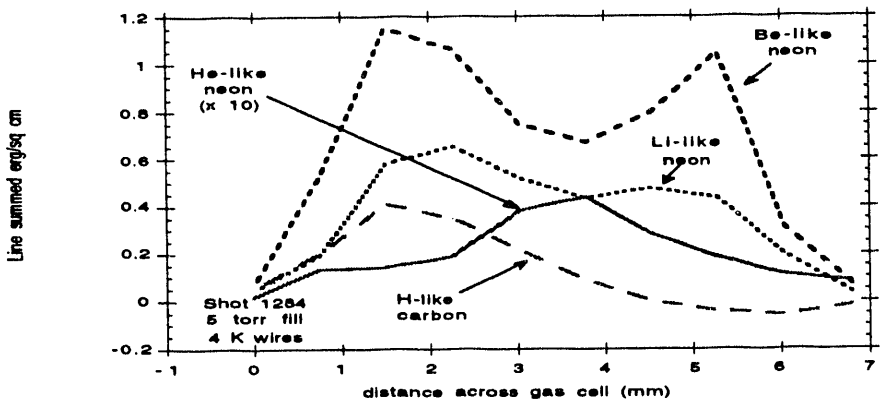

Figure 7. Spatial profiles of lines of various ionization states

The spatial distributions of lines of He-like, Li-like, and Be-like neon, and H-like carbon, recorded with a 10-nsec gate centered on the radiation power pulse are shown in figure 7. The lines are the 78.3-Å 3d-2p triplet transition for He-like neon, the 98.2-Å 3d-2p transition for Li-like neon, the cluster of 3d-2p triplet transitions around 110-Å for Be-like neon, and Balmer alpha at 182-Å for H-like carbon. The side window is located at position 0 in figure 7. Be-like and Li-like neon are seen to burn out at the center of the gas cell where He-like emissions peak. The neon could be heated by a radiatively driven shock wave that moves from the side window across the gas cell. The H-like carbon in figure 7 comes from the side window and its location of intensity fall-off could indicate the position of the shock. The shock is estimated to travel 1 mm during the 10-nsec data acquisition gate. The shock possibly heats a localized region of the neon, burning through the L shell and enhancing He-like neon in concert with direct photoionization.

As mentioned above, the He-like neon line measured is the 78.3-Å 3d to 2p triplet transition array. Modelling indicates that this line should be stronger than other He-like neon XUV lines because the lower 2p triplet level of this transition has a slow decay time and a large population. The small measured intensity of the 3d-2p He-like line points out the difficulty of measuring the candidate laser transition which is predicted to be about 10 times weaker in fluorescence.

We have measured the Li-like neon 5f-3d line to increase with neon fill pressure more rapidly than all other lines. The ratio of the 5f-3d intensity to that of the 5d-2p intensity is plotted versus neon fill pressure in figure 8. It is possible that the 5f-3d increase is due to lasing. Fill pressures of 30 torr often rupture the gas bag windows so that we have very little data at this high pressure.

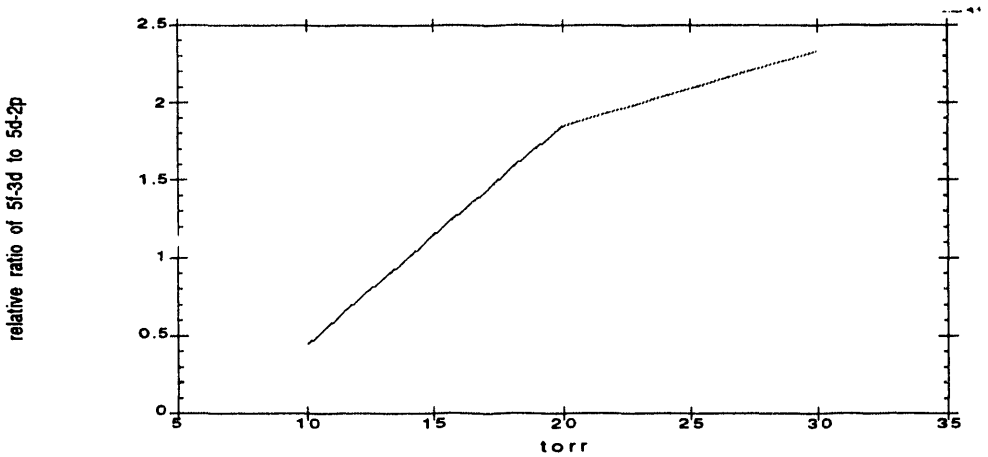

Figure 8. Increase of 5f-3d line intensity with fill pressure.

Radiation may not be the only mechanism by which the neon gas cell is heated. In figure 9 we show a time integrated spectrum from the neon gas cell recorded with the flat field spectrometer. The lines of Li-like neon are seen to have a "satellite" blue shifted by an amount proportional to the wavelength of the line. This is suggestive of a doppler shift, which would indicate jetting out of the neon gas cell at a very high velocity of 1.5e8 cm/sec. A possible mechanism for this acceleration is a J x B force, which would imply that the neon gas cell draws significant return current. The gas bag would need to draw tens of kiloamperes in radial current to accelerate to neon to these high velocities.

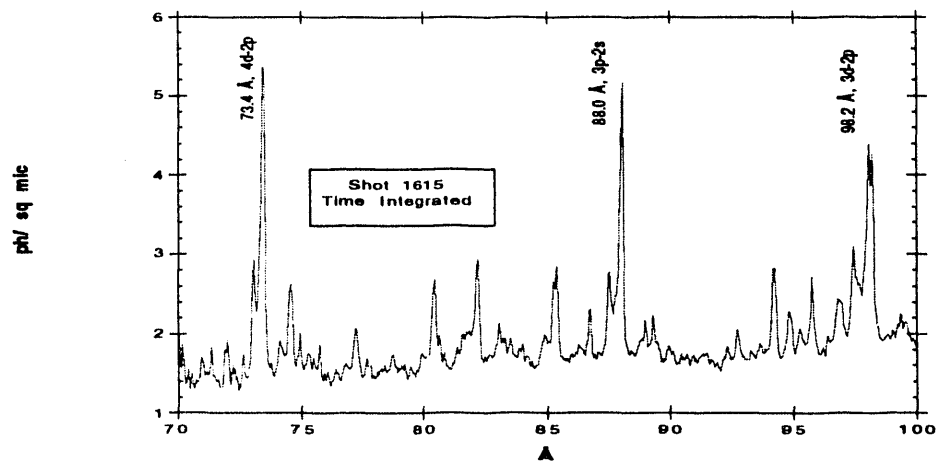

Figure 9. Li-like neon lines display blue shifted satellites that indicate plasma jetting likely driven by return current.

We have identified the 4d to 2p triplet transition in He-like neon due to the better sensitivity of the flat field instrument. The detected line is shown in figure 10. The relative intensity of this line with respect to the 3d to 2p triplet would indicate a 4 to 3 inversion[25] and corroborates the results of ref 22.

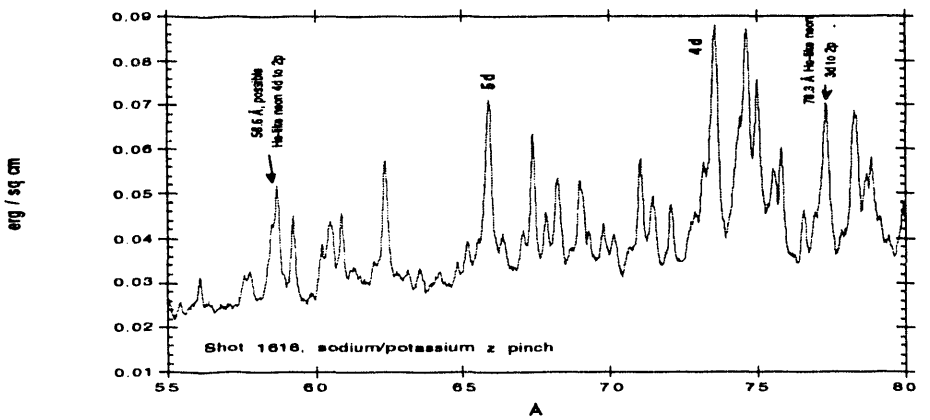

Figure 10. A line at 58.6 Å is identified as the He-like neon 4d-2p triplet transition.

The He-like lines are modelled to be due to keV pump radiation. In figure 11 we display the neon spectrum pumped by a gold spectrum which has comparitively less keV pump than a sodium/potassium pinch. With the gold pinch there are no He-like emissions. This particular shot, which is time resolved during the radiation pump, also shows an extreme amount of plasma jetting, again likely driven by current. The current, therefore, is incapable of exciting the He-like states. Evidently He-like lines can only be pumped by keV radiation.

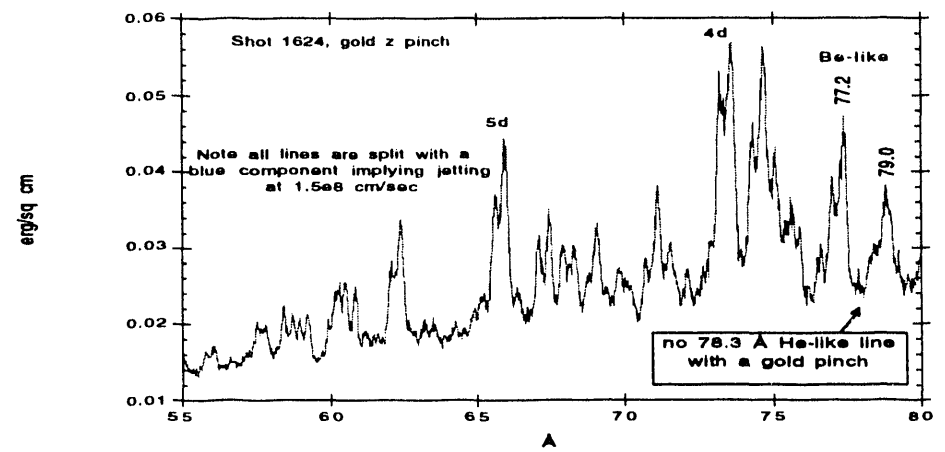

Figure 11. With the reduced keV pump of a gold pinch we see no emissions from He-like neon.

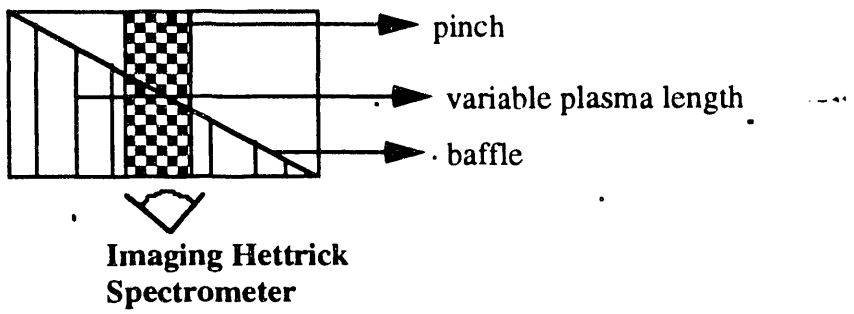

Figure 12. Geometry of single shot gain measurement attempt.

We have attempted a single shot gain length measurement. The geometry of the technique is shown in figure 12. The neon gas cell is diagonally baffled to only allow radiation to heat the plasma along a triangular portion of the neon. Viewed from below the flat field spectrometer images along a direction of increasing plasma length.

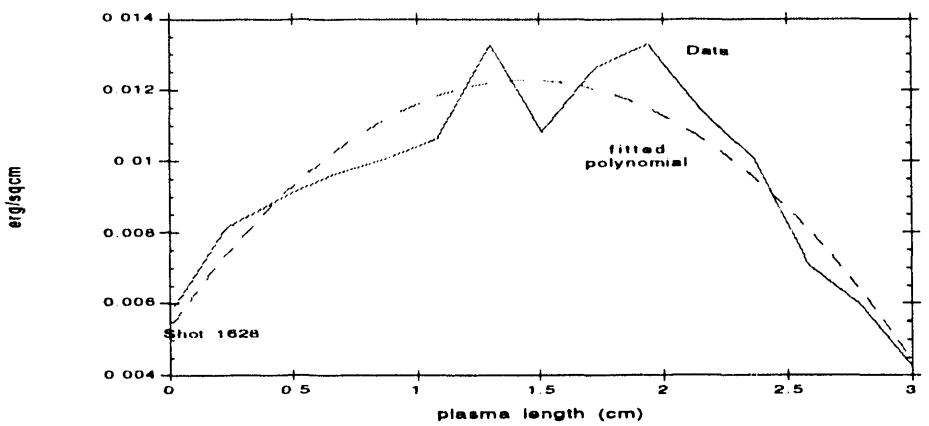

Figure 13. Intensity of Li-like neon 4d-3p line at 282.4 Å as a function of baffled plasma length.

The results from this experiment are rather discouraging as depicted in figure 13 which shows the intensity of a candidate recombination laser line as a function of plasma length. The line basically peaks along the center of the gas bag and falls off to either side. The profile suggest that the neon gas cell is not affected by the baffle, perhaps because it is heated by current, or because collisional processes or a diverging shock equilibrate the entire neon plasma even though only half of it is illuminated. The fall off of the Li-like neon line on either side of figure 13 is likely due to the cooling effect of the gas cell side walls. That the emissions peak along the center could also be suggestive of radiative self-pumping since most radiation source functions generally peak in the geometric center of the medium.

Besides having unwanted extra heating mechanisms the neon gas cell target is riddled with absorption problems due to the side walls and end window. The pinch side of the end window is shadowed from radiation and likely is not as hot as the rest of the end window. In figure 14 we show a time-gated neon spectrum revealing several candidate recombination

laser lines as recorded from the side window and gas cell center. Along the side window the 282.4-Å line is considerably absorbed with respect to harder 5 to 3 transitions below 200-Å. We could therefore expect lasing measurements above 200-Å along the side window to be unwise. Evidently the 282.4-Å line is too soft to transmit through the cool shadowed portion of the end window. However along the gas cell center, where the end window is well illuminated the 282.4-Å line is well transmitted. Here the 5 to 3 lines are weaker, likely because the recombinations peak near the higher densities of the side window. One final feature of figure 14 are very wide absorption lines from Li-like carbon. These have been indentified as coming from the gas cell target side wall. Indeed spatially resolved spectra show cool plama from these side walls limits the hot region of the neon gas cell to the central 2 mm, and it is possible that hot neon plasma measured to be localized to the gas cell center is more due to cooling by surrounding walls than to any localized heating effect.

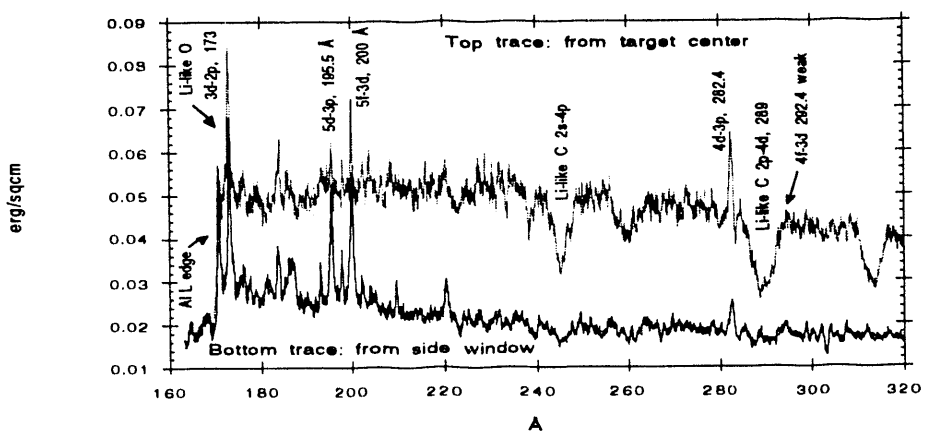

Figure 14. The 4d-3p line is absorbed by the shadowed portion of the end window. Wide C absorption lines indicate dense target side wall plasma.

4. CONCLUSIONS

We have measured the ionization balance across a neon gas cell irradiated by a 10-TW z-pinch. The measurements are consistent with a radiatively driven shock wave propagating through the neon. We have increased the overall level of ionization and the amount of He-like neon in the gas cell by introducing 25% potassium into the z-pinch load. This increases the ionizing soft x-ray radiation a factor of 3. Oxygen absorption lines have also been eliminated from the spectrum by using an oxygen-free 5000-Å thick polystyrene end window. From the measurement of fast plasma jetting and the lack of response of the neon plasma to a radiation blocking baffle we conclude that return current may be flowing in the gas cell. Current does not appear to affect the excitation of the He-like neon states because of the higher excitation energy required.

This work performed at Sandia National Laboratories supported by the U. S. Department of Energy under contract DE-AC04_76DP00789.

5. REFERENCES

1. D.L. Matthews, et al., Phys. Rev. Lett 54, 110 (1985)
2. M.D. Rosen, et al., Phys. Rev. Lett. 54, 106 (1985)
3. B.J. MacGowan, et al., Phys. Rev. Lett. 59, 2157 (1987)

4. T.N. Lee, E.A. McLean, and R.C. Elton, Phys. Rev. Lett. 59, 1185 (1987)
5. S. Suckewer, et al., Phys. Rev. Lett. 55,1753 (1985)
6. C. Chenais-Popovics, et al., Phys. Rev. Lett. 59, 2161 (1987)
7. P. Jaegle, et al., J. Opt. Soc. Am. B 4, 503 (1987)
8. D. Kim, et al., J. Opt. Soc. Am. B 6, 115 (1989)
9. J.C. Moreno, et al., Phys. Rev. A 39, 6033 (1989)
10. G. Jamelot, et al., Appl. Phys. B 50, 239 (1990)
11. V.A. Bhagavatula, J. Appl. Phys. 47, 4535 (1976)
12. J.P. Apruzese, et al., J. Appl. Phys. 53, 4020 (1982)
13. J.P. Apruzese and J. Davis, Phys. Rev. A 31, 2976 (1985)
14. J.P. Apruzese, et al., Phys. Rev. A 35, 4896 (1987)
15. F.C.Young, et al., Appl. Phys. Lett. 50, 1053 (1987)
16. J. Nilsen, Phys. Rev. 40, 5440 (1989)
17. B.N. Chichkov and E.E. Fill, Phys. Rev. A 42, 599 (1990)
18. Y.T. Lee, et al., J. Quant. Spectros. Rad. Transfer 43, 335 (1990)
19. J. Nilsen and E.A. Chandler, Phys. Rev. A 44, 4591 (1991)
20. J. Nilsen, J. Quant. Spectrosc. Radiat. Transfer 46, 547 (1991)
21. N. Qi and M. Krishnan, Phys. Rev. Lett. 59, 2051 (1987)
22. J.L. Porter, et al., Phys Rev. Lett. 68, 796 (1992)
23. J.P. Apruzese, et al., in Proceedings of the Second International Colloquium on X-ray Lasers, York, England, edited by G.J. Tallents (Institute of Physics, Bristol, 1991), p. 39
24. T.J. Nash, et al., Rev. Sci. Instrum. 61 2810 (1990)
25. J.P. Apruzese, private communication (1993)

DATE
FILMED
10/26/93
END